

OPEN ACCESS

Open Challenges on Aluminum Triflate-Based Electrolytes for Aluminum Batteries

To cite this article: Fatemehsadat Rahide *et al* 2023 *J. Electrochem. Soc.* **170** 030546

View the [article online](#) for updates and enhancements.

You may also like

- [Perspective—Are Rechargeable Aluminum Batteries with Aqueous Electrolytes Possible?](#)

Jasmin Smajic and Pedro M. F. J. Costa

- [Review—Open-Framework Structure Based Cathode Materials Coupled with Metallic Anodes for Rechargeable Multivalent Ion Batteries](#)

Ya Xiong, Yueqiang Lin and Qingzhong Xue

- [Graphite Oxide Cathode for Greener Rechargeable Aluminum Battery](#)

Zhanyu Li, Jianling Li, Yanying Liu et al.

Investigate your battery materials under defined force!
The new PAT-Cell-Force, especially suitable for solid-state electrolytes!



- Battery test cell for force adjustment and measurement, 0 to 1500 Newton (0-5.9 MPa at 18mm electrode diameter)
- Additional monitoring of gas pressure and temperature

www.el-cell.com +49 (0) 40 79012 737 sales@el-cell.com

EL-CELL[®]
electrochemical test equipment





Open Challenges on Aluminum Triflate-Based Electrolytes for Aluminum Batteries

Fatemehsadat Rahide,^{1,z}  Eugen Zemlyanushin,¹ Georg-Maximilian Bosch,² and Sonia Dsoke^{1,z} 

¹Institute for Applied Materials (IAM), Karlsruhe Institute of Technology (KIT), 76344 Eggenstein-Leopoldshafen, Germany

²Institute of Nanotechnology (INT), Karlsruhe Institute of Technology (KIT), 76344 Eggenstein-Leopoldshafen, Germany

Among possible “beyond Lithium” candidates, Aluminum is the most abundant one, and it can theoretically provide three times more charge per redox center as compared to Lithium. However, a drawback of Aluminum batteries is the requirement of an acidic electrolyte based on an ionic liquid and Aluminum chloride (AlCl_3) salts to enable plating and stripping. This electrolyte is very corrosive and restricts the use of suitable current collectors and all involved parts of the cell. Recently, Aluminum trifluoromethanesulfonate ($\text{Al}(\text{OTf})_3$) has been proposed as a non-corrosive alternative to AlCl_3 . It was suggested that this salt could enable plating and stripping of aluminum in a melt composed of urea and *N*-Methylacetamide (NMA). However, to assess the real suitability of these electrolytes, it is necessary to evaluate their electrochemical behavior at different working conditions. With this purpose, we present the electrochemical study of two electrolyte compositions based on the non-corrosive $\text{Al}(\text{OTf})_3$ salt, urea and two different solvents, NMA and Ethyl-Isopropyl-Sulfone (EIPS). This work highlights important challenges related to the reversibility of the redox reactions when using $\text{Al}(\text{OTf})_3$ -based electrolytes and reveals an unexpected behavior with substrates other than Pt or Cu. These aspects should be taken into consideration in future research for AlCl_3 -free electrolytes.

© 2023 The Author(s). Published on behalf of The Electrochemical Society by IOP Publishing Limited. This is an open access article distributed under the terms of the Creative Commons Attribution 4.0 License (CC BY, <http://creativecommons.org/licenses/by/4.0/>), which permits unrestricted reuse of the work in any medium, provided the original work is properly cited. [DOI: 10.1149/1945-7111/acc762]



Manuscript submitted December 20, 2022; revised manuscript received March 10, 2023. Published April 4, 2023.

Supplementary material for this article is available [online](#)

Rechargeable Lithium-ion batteries (LIBs) are the established technology dominating the electrochemical energy storage market. Metallic Lithium (Li) has a notable volumetric capacity (2062 mAh cm^{-3}) and the highest gravimetric capacity among alkali metals (3857 mAh g^{-1}).^{1,2} However, the high cost and low abundance of Li (0.0065% of the Earth’s crust) push scientists to find alternatives. Aluminum (Al) is far more abundant ($\sim 8\%$ of the Earth’s crust mass fraction) than Li and has about four times higher volumetric capacity than Li ($8040 \text{ vs } 2062 \text{ mAh cm}^{-3}$).^{3,4} Therefore, rechargeable Aluminum Batteries (RABs), with metallic Al as an anode, appear promising for sustainability and energy density reasons. Depending on the electrolyte, RABs are classified into aqueous and non-aqueous ones.⁵ However, it is well-known that aqueous systems impede the use of an Al foil negative electrode, as hydrogen evolution occurs at potentials higher than that of Al plating. The negative standard reduction potential of Al anode occurs at -1.662 V vs SHE .⁵ On the other hand, ionic liquids (IL)-based electrolytes, with their nonvolatile and nonflammable properties, are the most common non-aqueous electrolytes.⁵ The most popular ionic liquid-based electrolyte for RABs is a mixture of AlCl_3 with 1-Ethyl-3-methylimidazole chloride (EMImCl). Depending on the molar ratio between the two components, the Al species mainly exist as monovalent complex anions, including $[\text{Al}_2\text{Cl}_7^-]$ and $[\text{AlCl}_4^-]$.⁶ Unfortunately, the strong coordination of Al^{3+} and Cl^- hampers the existence of Al^{3+} .⁵ With IL-based electrolytes, depending on the positive electrode material used, different charge carriers are involved (e.g., AlCl_4^- , AlCl_2^+ , AlCl_2^+), often resulting in a “dual ion” storage mechanism rather than on Al-ion shuttling.⁷ Generally, during charge and discharge, $[\text{Al}_2\text{Cl}_7^-]$ converts to Al^{3+} and $[\text{AlCl}_4^-]$ and vice versa.^{8,9} One of the most critical issues is that such IL- AlCl_3 -based electrolytes are corrosive and aggressive, which limits the choice of possible cathode materials and auxiliary parts of the battery (e.g., binders, separator, current collector and battery casing).¹⁰ The corrosivity of the chloroaluminate-based ILs associates with the existence of Cl^- in $[\text{Al}_2\text{Cl}_7^-]$ and $[\text{AlCl}_4^-]$ species, and also with the Lewis acidity of the species in solution, which depends on the molar ratio between AlCl_3 and the IL.

Moreover, AlCl_3 makes the electrolyte highly sensitive to moisture.^{8,9,11}

Slim and Menke¹² determined how Cl^- affects the electrochemistry and Al speciation in $\text{Al}(\text{OTf})_3/\text{THF}$, $\text{Al}(\text{OTf})_3$ plus LiCl in THF, and AlCl_3/THF systems using theoretical and experimental methods. They assert that Cl^- considerably increases the electrochemical activity of Al-ions by enabling easy Al plating. However, Cl^- makes the electrolyte corrosive.¹²

Considering these serious drawbacks, it is urgent to discover novel electrolytes, possibly chloride-free. Properties of an electrolyte include: high conductivity, low viscosity, and a large electrochemical stability window. Unfortunately, the high charge density of the Al^{3+} cation results in very strong Coulombic interaction with the corresponding counter anions, which reduces the solubility of Al-salts in common organic solvents.¹⁰ Therefore, the ionic conductivity of Al-based electrolytes is relatively low. Recently, $\text{Al}(\text{OTf})_3$ and $\text{Al}(\text{TFSI})_3$ have been proposed as a non-corrosive alternative salt to AlCl_3 .^{13–15} $\text{Al}(\text{TFSI})_3$ in acetonitrile (AN) has been proposed by Chiku et al.¹⁵ as a new chloride-free electrolyte medium that can achieve a broad electrochemical window and a low overpotential for the deposition or dissolution of aluminum. $\text{Al}(\text{TFSI})_3$ in AN has an electrochemical window of roughly 3.6 V, which is larger than the electrochemical window of traditional ionic liquid electrolytes (2.5 V).¹⁵

By combining AlCl_3 with certain ligands, Mandai and Johansson¹⁶ synthesized and presented a variety of cationic aluminum coordination complexes. They found that the replacement of MIm by BIm in $[\text{Al}(\text{alkylimidazole}(\text{RIm}))_6][\text{TFSI}]_3$, where R can be butyl or methyl, results in the room temperature molten cationic Al-solvated quasi-IL. They reported that $[\text{Al}(\text{BIm})_6][\text{TFSI}]_3$ as a novel and non-moisture-sensitive aluminum-based quasi-ionic liquid, shows both cathodic and anodic current due to the deposition and dissolution of Al metal, respectively.¹⁶

Wang et al.¹³ used IL electrolyte obtained by mixing 1-Butyl-3-methylimidazolium trifluoromethanesulfonate ($[\text{BMIM}]\text{OTf}$) with the corresponding aluminum salt ($\text{Al}(\text{OTf})_3$). Their study reveals that $\text{Al}(\text{OTf})_3/[\text{BMIM}]\text{OTf}$ IL electrolyte has a wider electrochemical stability window than the $[\text{EMImCl}]/\text{AlCl}_3(1:1.5)$ -based one, with anodic stability up to 3.25 V vs Al^{3+} on Glassy Carbon (GC) electrode. Nevertheless, it is proven that the increase of $\text{Al}(\text{OTf})_3$

^zE-mail: fatemehsadat.rahide@kit.edu; sonia.dsoke@kit.edu

concentration results in a pairing phenomenon, which in turn leads to the increase of conductivity, and the decrease of the electrolyte's viscosity.¹³ In a study by Reed et al.,¹⁷ the physicochemical characteristics of Al(OTF)₃ in 2-methoxy-ethyl ether diglyme were reported experimentally and computational findings from Density Functional Theory (DFT) calculations were compared. According to DFT calculations, they reported that the electrochemical window varies from 7.2 V for neat diglyme to 3.5 V for highly concentrated electrolytes. In addition, it is reported that the oxidative stability of the triflate and the reductive stability of the [Al(diglyme)₂]³⁺ complex control the cathodic and anodic edges of the window.¹⁷

Mandai and Johansson¹⁸ studied a series of room-temperature ternary electrolytes based on mixtures of Al(OTF)₃, NMA, and urea. In these mixtures, the conductivity, which depends on the interactions between the multivalent metal cations and the corresponding counter anion, can be improved by properly modifying the amount of urea. As a result of this study, the most suitable molar ratio of urea/NMA/Al(OTF)₃, which provides the optimum ionic conductivity value (i.e., $2.5 \times 10^{-3} \text{ Scm}^{-1}$), and strong solvation ability, is 0.19/0.76/0.05.¹⁸ This selected formulation was electrochemically tested by Mandai and Johansson on a Pt electrode, highlighting a possible Al plating and stripping. However, a further electrochemical study is necessary in order to fully assess the suitability of this electrolyte formulation for Al batteries. On the other hand, exploring other sustainable solvents that can replace the harmful NMA is also necessary. With this respect, sulfones are a class of solvents that would have a weak coordination strength with Al³⁺. Early work on Aluminum deposition demonstrates that aluminum can be plated in dimethyl sulfone ((CH₃)₂SO₂) and AlCl₃.¹⁹ Nevertheless, due to the high melting point of dimethyl sulfone, electrochemical plating is possible only at temperatures higher than 100 °C. Linear sulfones have been explored as solvents for supercapacitors²⁰ and for Li-ion and Mg-ion batteries.^{21,22} Only one work reports the use of Ethyl-Isopropyl-Sulfone (EiPS) in Aluminum batteries.²³ The authors of this work attempted to eliminate the corrosive AlCl₃ by substituting it with Al(BF₄)₃ without success. This work highlights and claims that the presence of AlCl₃ is fundamental for Aluminum plating and stripping. However, it is important to consider that the BF₄⁻ anion can form a stable passivating layer on the surface of the negative electrode,²⁴ which can block any further Aluminum plating and stripping. Among other sulfone-type solvents, like ethyl isobutyl sulfone (EiBS) or isopropyl-s-butyl sulfone (iPsBs), the linear EiPS shows the lowest viscosity and a high permittivity. This is probably caused by a greater interaction between the more branched alkyl chains.¹³ The same effect was investigated by Das et al.²⁵ for room-temperature ionic liquids. EiPS has a low melting point (−8 °C) and a high boiling point (265 °C), making it a suitable solvent. The low melting point of EiPS has a correlation with its viscosity, which is due to the weak intermolecular force of EiPS.²⁰ Moreover, EiPS has good thermal stability with no significant degradation or evaporation up to 85 °C.²⁶ Its high stability is due to its low reactivity with H₂O.²⁰ It is reported that pure EiPS has an electrochemical stability window (ESW) of 3.7 V²⁰ and even 3.9 V.²⁶ Furthermore, the reported sulfone-based electrolyte consisting of the mixture of AlCl₃ and dialkylsulfone exhibited an exquisite performance, including no corrosion and no Aluminum dendrite formation, as well as relatively good charge/discharge capacity in RABs²³. An ideal electrolyte should have a suitable solvent with a solvating power to form a liquid electrolyte at room temperature. It is reported that acetamide and urea mixtures have optimum solvation properties, being able to dissolve salts of divalent metal ions like Mg[OTF]₂.²⁷ Since there are many analogies between Mg and Al in terms of the electrochemical properties, this knowledge can be transferred to Al-batteries. The desired solubility is related to the capability of the carbonyl- and primary amino groups to coordinate with different cations and anions. These kinds of coordination lead to salt dissociation by relaxation of hydrogen-bond interactions between the organic compound and ion-ion interactions. Moreover, the deformation of the hydrogen bonds influences the bond strength,

which should also result in a Raman frequency shift and lower thermal stability. However, a too strong coordination bond, which is too hard to break, gives rise to a large polarization resulting in a large overpotential.²⁷

Inspired by the mentioned works on chloroaluminate-free electrolytes, we conducted an electrochemical investigation of two electrolyte compositions based on the Al(OTF)₃ salt, specifically, on a composition based on urea/NMA/Al(OTF)₃ and another one based on urea/EiPS/Al(OTF)₃. By systematically varying conditions such as temperature, and electrode substrates, we revealed important challenges, which are hampering the use of these “non-corrosive” electrolytes on real Al batteries.

Experimental

Materials.—In this study, Ethyl Isopropyl sulfone (EiPS) (97.00%) was purchased by TCI. Aluminum trifluoromethanesulfonate (Al(OTF)₃) (99.9% trace metal basis), *N*-methylacetamide (NMA) (99%), urea (99%) were all purchased from Sigma-Aldrich. Al(OTF)₃ and urea were dried in a glass oven (BÜCHI Glass Oven B-585) under vacuum at 80 °C for 48 h and then stored in an Argon-filled glovebox (MBraun, <0.5 ppm O₂, <0.5 ppm H₂O) before being used. Molecular sieves (MS) of 3 Å (beads, 4 – 8 mesh) were purchased from Sigma-Aldrich. EiPS was dried with MS for 10 days at room temperature till the water content became less than 25 ppm. NMA was firstly melted at 40 °C and then dried with MS until the water content was less than 25 ppm. Urea/NMA/Al(OTF)₃ ternary electrolyte (NMA-based electrolyte) with a final molar ratio of 0.19:0.75:0.05 was prepared first by melting NMA at 40 °C.¹⁸ Then the appropriate amounts of dried Al(OTF)₃ and urea were added and stirred for 12 h at room temperature inside the glovebox. The second electrolyte based on urea/EiPS/Al(OTF)₃ (EiPS-based electrolyte), with a molar ratio of 0.30:0.65:0.05 based on better solubility, was prepared by mixing the appropriate amounts of Al(OTF)₃ and EiPS and adding the required amounts of urea. The mixture was stirred for 12 h at the ambient temperature inside the glovebox. The EiPS-based electrolyte has been prepared considering the ability to form Al³⁺ complex with six surrounding urea molecules.^{28–30} Therefore, due to the 1:6 metal-to-ligand molar ratio between urea and Al(OTF)₃, the molar ratio of 0.30:0.65:0.05 was chosen for EiPS-based electrolyte. Based on our experience, the 1:7 metal-to-ligand molar ratio results in a solubility issue. To calibrate the reference electrode, electrolytes containing Ferrocene (0.02 mol⁻¹) as an internal reference were prepared. Ferrocene (98.00%) was purchased from Sigma-Aldrich. The Aluminum foil (0.075 mm thickness and 99.0% purity), Titanium foil (0.025 mm thickness and 99.6% purity), and Molybdenum foil (0.025 mm thickness and 99.9% purity) were purchased from Goodfellow. The Platinum foil (0.4 mm thickness and 99.9% purity) was supplied from rhd Instruments GmbH & Co. KG (Germany). Copper foil (9 μm thickness and > 99.8% purity) was purchased from MTI corporation.

Physical characterization.—The physical properties of the NMA-based electrolyte are reported in the work of Mandai and Johansson.¹⁸ The EiPS-based electrolyte was characterized with respect to density, viscosity, and ionic conductivity in temperatures ranging from 20 to 80 °C. To measure density (δ) and viscosity (η), a DMA 4100 (Anton Paar) viscosimeter was used. Temperature-dependent ion-conductivity of the EiPS-based electrolyte solution has been calculated using electrochemical impedance spectroscopy (EIS). A TSC 1600 closed measuring cell (with a cell constant (K_{cell}) of 1.3 cm⁻¹) in combination with a Microcell HC setup (rhd instruments GmbH & Co. KG) was used to carry out electrochemical impedance spectroscopy for the determination of the conductivity.³¹ The cell was filled with 1.0 ml of sample solution inside the glovebox. After being sealed, the cell was transferred to the test station (cell stand) outside of the glove-box. The Microcell HC temperature was used to enable an automated adjustment of the temperature by using a Peltier element technique, with a 0.1 °C

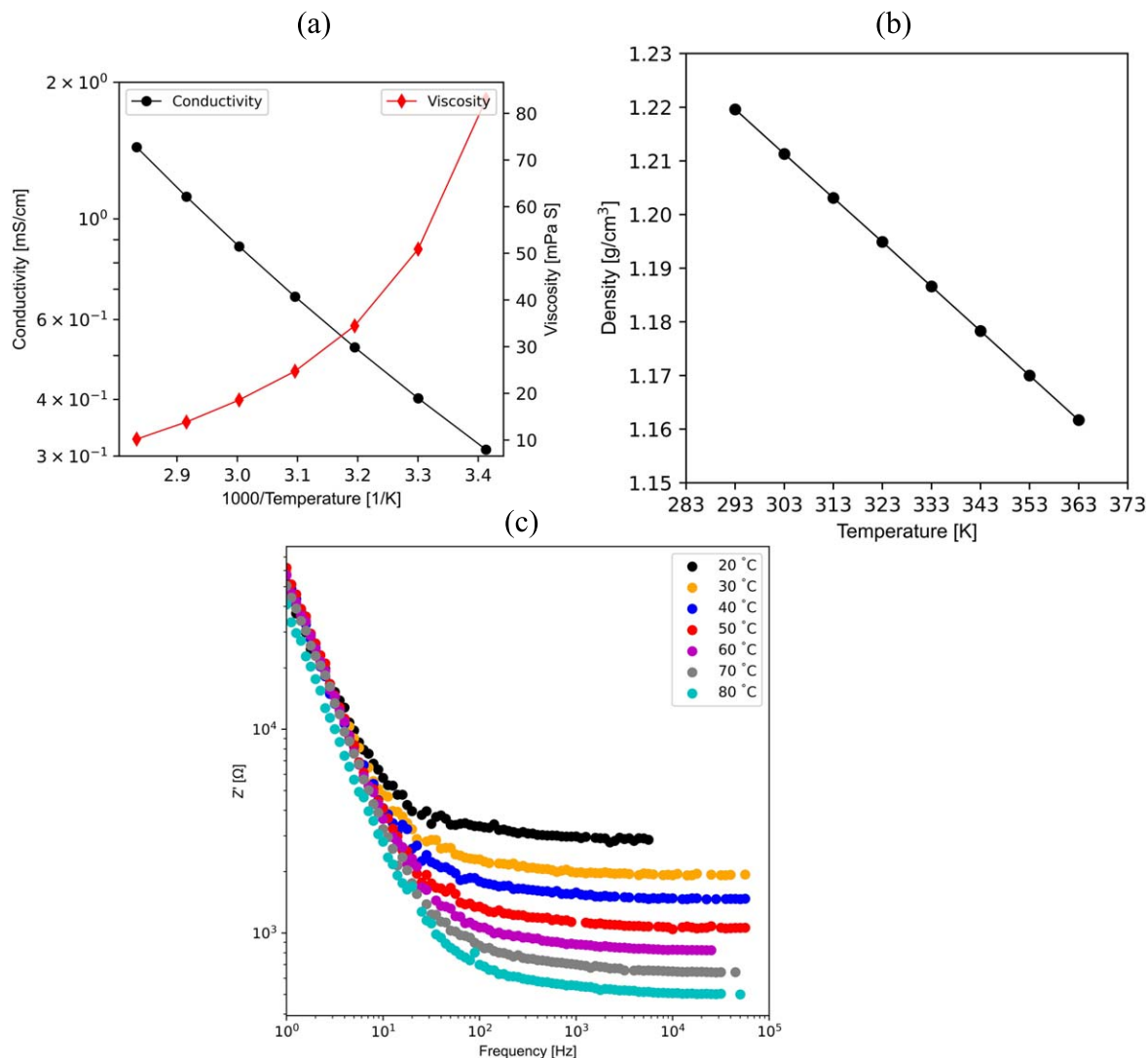


Figure 1. (a) Arrhenius plots of the ionic conductivity σ and viscosity η (b) Density ρ in the 20–80 °C range of urea/EiPS/Al(OTF)₃ (c) Impedance spectra in the form of Bode plots.

Table I. Physicochemical properties of Al(OTF)₃-base electrolytes at 30 °C.

	ρ [g/cm ³]	η [mPa.s]	σ [mS cm ⁻¹]	ϵ_r solvent
urea/NMA/Al(OTF) ₃ ¹⁸	1.11	33.4	2.4 at 30 °C	178 at 30 °C ³²
urea/EiPS/Al(OTF) ₃	1.21	50.90	0.4 at 30 °C	55 at 25 °C ²⁰

Table II. Melting and boiling points of the electrolyte components.

	Melting point [°C]	Boiling point [°C]
N-Methylacetamide (NMA) ³⁶	27	205
1-Ethyl isopropyl sulfone (EiPS)	-8 ²⁰	265 ²⁰
urea	133 ³⁷ (decomposition)	—
Aluminum trifluoromethane sulfonate (Al(OTF) ₃)	300	N/A

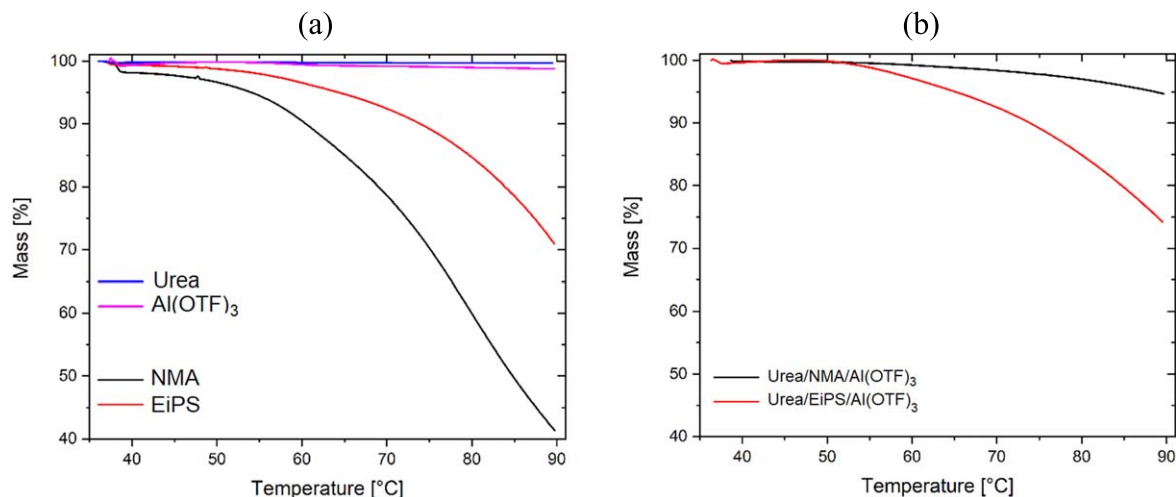


Figure 2. TGA of (a) the pure chemicals and (b) the two electrolyte mixtures. The measurement was done between 35 and 90 °C with a heating rate of 1 K min⁻¹.

accuracy. The EIS measurements were performed with a Biologic VMP potentiostat (France) equipped with EC-Lab software. Impedance data were evaluated using the RelaxIS 3^o software suite (rhd instruments GmbH & Co. KG). Impedance spectra were recorded for frequencies ranging from 1 Hz to 100 KHz (20 points per decade) with an AC voltage amplitude of 10 mV at several temperatures (20 °C–80 °C with 10 °C intervals). A 0.5 h hold time was set after reaching the temperature set-point before starting the EIS experiment to ensure the thermal equilibrium of the system. Thermogravimetric Analysis (TGA) and Fourier-transform infrared spectroscopy (FT-IR) of the electrolytes were recorded using Bruker Tensor 27 FT-IR spectrometer. All measurements were carried out inside the Argon-filled glovebox.

Electrochemical setup.—All electrochemical experiments were performed in an airtight and sealed TSC1600 cell (Fig. S1). The measuring cell (TSC1600 closed cell from rhd Instruments) is equipped with a Platinum crucible, which functions as a sample container and counter electrode. The Pt is an auxiliary counter electrode with a very large surface area that can support the current generated at the WE. The electrolyte is in large excess with a volume of 1.0 ml. With this configuration, the distance between the counter and working electrode is maximized to minimize the effects of oxidative reaction products formed at the CE on the processes taking place at the WE during the first reduction (plating) process.

Glassy Carbon (GC) and Platinum (Pt) discs working electrodes (WE, with a geometric area of 0.07 cm²) and a Silver (Ag) wire quasi-reference electrodes were polished, respectively, with 250 nm diamond polishing paste, and 1 μm diamond suspension before being used in experiments. The Al quasi-reference electrode was further soaked in a mixture of H₂SO₄/H₃PO₄/HNO₃ (25/70/5 by volume) for 5 to 15 min to remove any dirt or residual oxide.¹⁸ Then, the Al quasi-reference electrode was washed with acetone and dried under vacuum immediately before the measurements. Linear sweep voltammetry (LSV), with a scan rate of 5 mVs⁻¹, was used to determine the anodic stability of the electrolyte on two different electrode substrates, Pt and GC on the TSC1600 closed cell with an Ag wire as a reference electrode. Cyclic voltammetry (CV) was recorded with a scan rate of 20 mVs⁻¹. The Microcell HC cell stand allows the establishment of the cell connections to the potentiostat. The measuring TSC surface cell from rhd instruments (Fig. S2) was used for investigating metal foils as working electrodes (anodes) in contact with a liquid electrolyte. TSC surface cell is based on a gold-plated thermo-block with an integrated Pt100 temperature sensor. The loaded cell was sealed by a PEEK housing that allows for performing the test of air- and moisture-sensitive samples. The well-

polished GC and Pt discs (6 mm radius) were used as counter electrodes, Ag and Al wires as quasi-reference electrodes and Pt, Mo, Al, Ti foil were used as working electrode substrates. The temperature-dependent ion-conductivity of the EiPS-based electrolyte was determined with the aid of electrochemical impedance spectroscopy.

Results and Discussion

Physical properties of the electrolyte.—Figures 1a and 1b depict the ionic conductivity of EiPS-based electrolyte as well as its viscosity and density in the temperature range of 20 to 80 °C. Figure 1c presents the temperature-dependent impedance spectra as Bode plots (the impedance (*Z*) vs the measuring frequency (*f*)). The plateau value denotes the bulk resistance for ion movement. By increasing the temperature, the plateau value decreases owing to the increase in conductivity of the electrolyte. Density and viscosity values are provided in Table SI.

The corresponding physical parameters for the NMA-based electrolyte are reported in the paper of Mandai and Johansson.¹⁸ For common electrolytes, the conductivity is proportional to viscosity; nevertheless, NMA-based electrolyte owns high conductivity despite its high viscosity and low fluidity. The optimum ionic conductivity value of urea/NMA/Al(OTF)₃ (0.19/0.76/0.05) is 2.5×10^{-3} Scm⁻¹ at 30 °C.¹⁸ In comparison to NMA-based electrolytes, the EiPS-based electrolyte (0.65/0.05:0.30) has a conductivity of 0.38 mS cm⁻¹ at 30 °C. In summary, EiPS-based electrolyte shows high viscosity, resulting in low ionic conductivity, while urea/NMA/Al(OTF)₃ (0.19/0.76/0.05) has high conductivity, despite the high viscosity.¹⁸

Solvents with a high dielectric constant (ϵ_r) moderate the induced powerful electric field of charged species, consequently weakening salt dissociation and the ion-ion interactions.³² The ionic conductivity dictates the charge transport rate of the active ions. The small (ionic radius of 0.050 nm) and trivalent Al³⁺ ion with a strong electric field affect the polarization of the solvated ions. In addition, in terms of ternary electrolytes, dissociation has a strong correlation with the composition. For instance, it was proved that a minor substitution of NMA by urea diminishes the Al(OTF)₃ dissociation, whereas additional substitution enhances salt dissociation.¹⁸ NMA, as one of the most self-associated liquids, possesses high static dielectric constant and high conductivity among other molecular liquids.³² Regarding the NMA-based electrolyte, NMA operates as a solvent for Al(OTF)₃; therefore, a small substitution of NMA by urea surprisingly promotes the Al(OTF)₃ dissociation. However, a mixture of NMA and urea possesses a lower dielectric constant ($\epsilon_r = 81.3$) than pure NMA ($\epsilon_r = 178$).^{18,32} Urea affects the

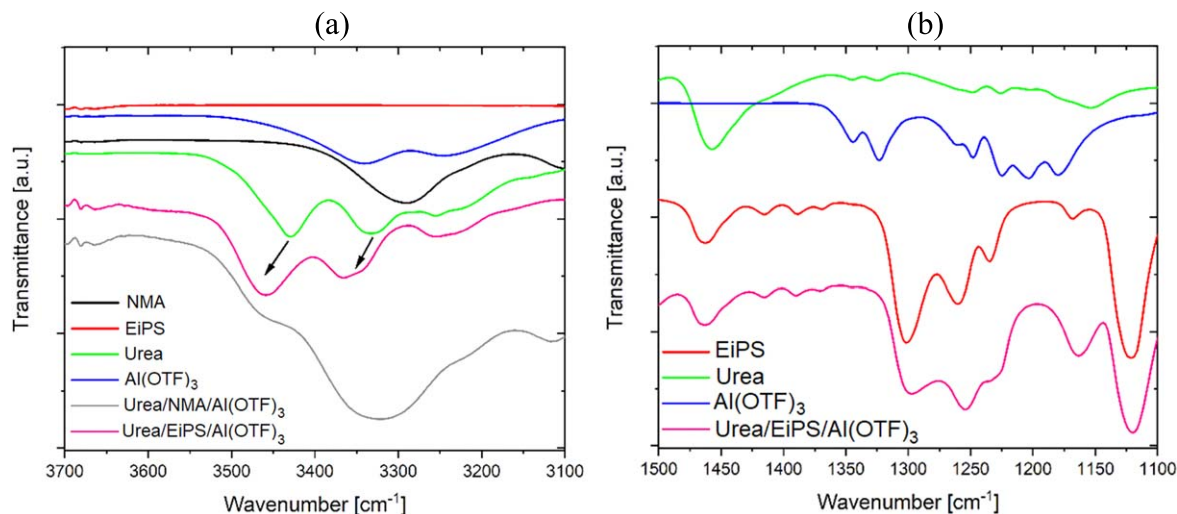


Figure 3. FT-IR spectra of the pure substances and the two electrolyte mixtures in the range for (a) N-H vibration bands for the two electrolyte compositions and (b) S=O vibration bands for the Urea/EiPS/Al(OTF)₃ mixture.

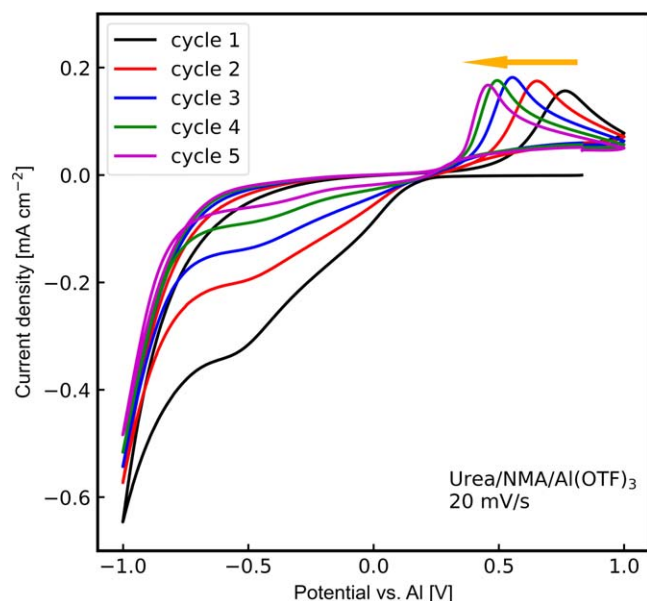


Figure 4. Cyclic voltammograms recorded with the scan rate of 20 mVs⁻¹ on a Pt disc as a working electrode and Al quasi reference as a reference electrode in urea/NMA/Al(OTF)₃. The cell used was a TSC 1600 closed cell.

properties of NMA, but its role is still a matter of discussion.^{18,33,34} Urea allows for further dissociation of Al(OTF)₃ salt-solvent complex, which refers to the bidentate hydrogen bonding of urea with OTF⁻ in deep eutectic solvents.³⁵ In comparison, at 25 °C pure EiPS ($\epsilon_r = 55$) has a lower dielectric constant than pure NMA. Accordingly, higher ionic conductivity is expected for NMA-based electrolytes.^{20,32} EiPS has a rather low melting point of -8 °C, and a high boiling point of 265 °C with a viscosity of 5.6 mPa.s at 25 °C,²⁶ while NMA's melting point ranges from 26 to 28 °C, with a high boiling point (204 °C–206 °C).³⁶ Therefore, we assume EiPS has a wider operable temperature window compared to the NMA-based one. It is also reported that at 20 °C the electrolyte containing 100% EiPS has a viscosity of 12.3 mPa.s with a conductivity of 3.5 mS cm⁻¹.²⁶ In Brief, Although the EiPS-based electrolyte has lower ionic conductivity and high viscosity, it possesses high thermal stability due to a wider working temperature window. The physicochemical properties of Al(OTF)₃-base electrolytes are presented in Table I.

Intermolecular interactions and thermal stability of the electrolyte.—As mentioned above, the intermolecular interactions in ternary solvents affect ion mobility and conductivity. Therefore, the interaction of the different substances was investigated by thermogravimetric analysis (TGA) coupled with differential scanning calorimetry (DSC) and Fourier Transform Infrared Spectroscopy (FT-IR). Moreover, in principle, thermal analysis is important to understand the thermal stability of the electrolyte components.

Table II shows the melting and boiling points of the four components. NMA, EiPS, urea, and Al(OTF)₃. NMA and EiPS are liquid at the starting conditions of the TGA-DSC measurement (35 °C of ambient temperature), while urea and Al(OTF)₃ are solid.

Figure 2a shows a TGA measurement of the four chemicals from 35 to 90 °C with a relatively slow heating rate of 1 Kmin⁻¹. It can be seen that the two solid chemicals (urea and Al(OTF)₃) show no weight loss over the whole temperature range due to their high thermal stability. NMA and EiPS, on the other hand, show a continuous decrease in mass over the temperature range and have not yet reached their boiling point, a loss of mass occurs.

The DSC measurement (Figs. S3-a and S3-b) does not show any decomposition of the substances. The mass loss can be explained by the continuous gas flow circulating around the sample during the TGA measurement, thus enabling continuous material removal in the gas phase. This mass loss should be, therefore, correlated to evaporation due to the constant concentration balance in the gas phase above the liquid. Since the vapor pressure reflects the intermolecular interactions of components in a solution, it is possible to infer the strength of the interactions between the molecules from the mass loss under the same conditions. The mass loss of NMA is almost two times higher than that of EiPS (Fig. 2a). This is also in agreement with the boiling points of the two liquids reported in Table II. Accordingly, the NMA molecules have a weaker intermolecular interaction than the molecules of EiPS, which can be explained by additional van-der-Waals interactions between the isopropyl and ethyl groups in EiPS.

Figure 2b shows a TGA of the electrolyte mixtures measured in the same conditions as the single components. Also in this case, for both samples, a continuous decrease in mass is observed. In contrast to the measurement of the pure substances, the mixture based on NMA shows a significantly lower mass loss of only 5%. On the other hand, the electrolyte with EiPS shows a strong mass loss of 26%. Since the level of evaporation in the mixture is significantly reduced compared to the pure NMA, it can be concluded that the intermolecular interactions are strengthened by adding the other two

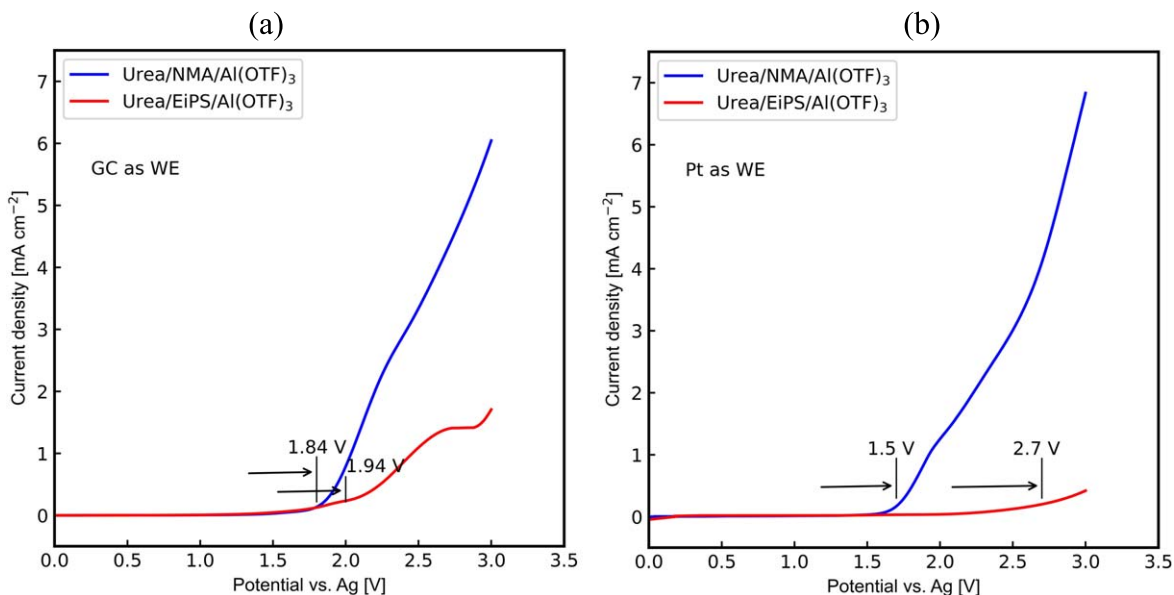


Figure 5. LSV for AlCl_3 -free electrolytes at $25\text{ }^\circ\text{C}$ on a TSC1600 closed cell recorded on (a) a GC disc at the scan rate of 10 mVs^{-1} and (b) a Pt disc at the scan rate of 5 mVs^{-1} . Ag wire was used as a quasi-reference electrode.

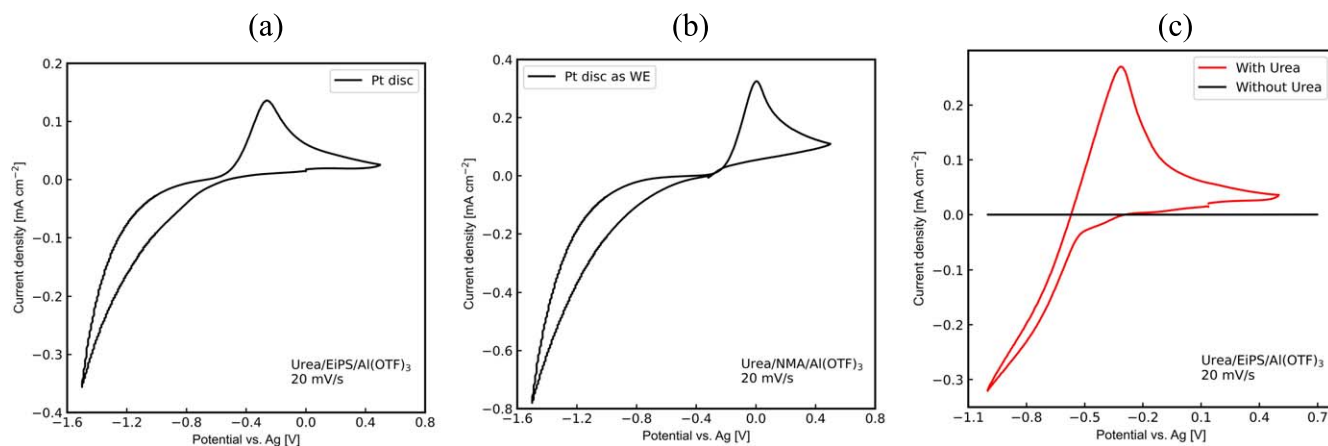


Figure 6. Cyclic voltammograms were recorded on a Pt disc in TSC1600 cell in (a) urea/NMA/Al(OTF)₃ (b) urea/EiPS/Al(OTF)₃. (c) urea/EiPS/Al(OTF)₃ and EiPS/Al(OTF)₃. Ag wire is used as quasi-reference electrodes.

components (urea and $\text{Al}(\text{OTF})_3$). In contrast, no significant changes in mass loss can be observed comparing the EiPS electrolyte mixture with the pure EiPS. This result points to the fact that there are no strong intermolecular interactions between EiPS and the other two substances in the ternary electrolyte, leading to no changes in the vapor pressure. As mentioned earlier, NMA can interact with the trivalent Al^{3+} ion and solvate it very well. In addition, NMA can form hydrogen bonds with urea and also provide an intermolecular interaction.¹⁸ In this way, the high charge concentration of the Al^{3+} ion will be distributed over the solvent. According to previous studies, the strong Al–O bond in $[\text{Al}(\text{EiPS})_3]^{3+}$, whose structure was confirmed by Y. Nakayama et al.,²³ would prevent the Al plating. The strategic addition of urea leads to a weakening of Al–EiPS interaction with the formation of a hybrid complex with urea, which is expected to be electrochemically active.

Figure 3 shows the FT-IR spectra of the two electrolyte mixtures compared with the pure components, while the full spectra can be seen in the supporting information file (Figs. S4-a and S4-b). The interactions of urea, NMA and EiPS with Al^{3+} and their mixtures were considered.

It is known that urea solvates Al^{3+} cations, establishing a coordinative bond via the free electron pairs of oxygen.³⁰ This

formally transfers an electron from oxygen to the Al^{3+} cation, thus lowering the electron density at the oxygen.³⁰ This results in a shift of the electron density in the urea molecule and leads to a stronger attraction of the protons to the nitrogen atoms. The increased binding of the amino groups can also be seen in the FT-IR spectrum and can thus serve as an indicator of the coordination of urea to Al^{3+} . The vibrational bands of these N–H bonds can be seen in the range of 3600 and 3200 cm^{-1} .³⁸ Fig. 3a shows a comparison of the two electrolytes as well as of the pure chemicals. The bands of pure urea of the N–H vibration at 3425 and 3325 cm^{-1} are shifted to higher wavenumbers as the intermolecular interaction in the two electrolyte mixtures leads to the Al-complex formation and strengthening of the binding. A similar interaction can also be assumed for NMA. However, since the bands of NMA and urea overlap to a large extent, no clear statement can be made.

A similar interaction as that of the C=O group of urea with the Al^{3+} cation can also be assumed for the S=O groups. Figure 3b shows the corresponding range of the FT-IR spectrum from 1500 to 1100 cm^{-1} . In contrast, no shift in the vibrational bands for EiPS and thus no strong interaction between the S=O groups and Al^{3+} is evident when urea is present in the mixture.

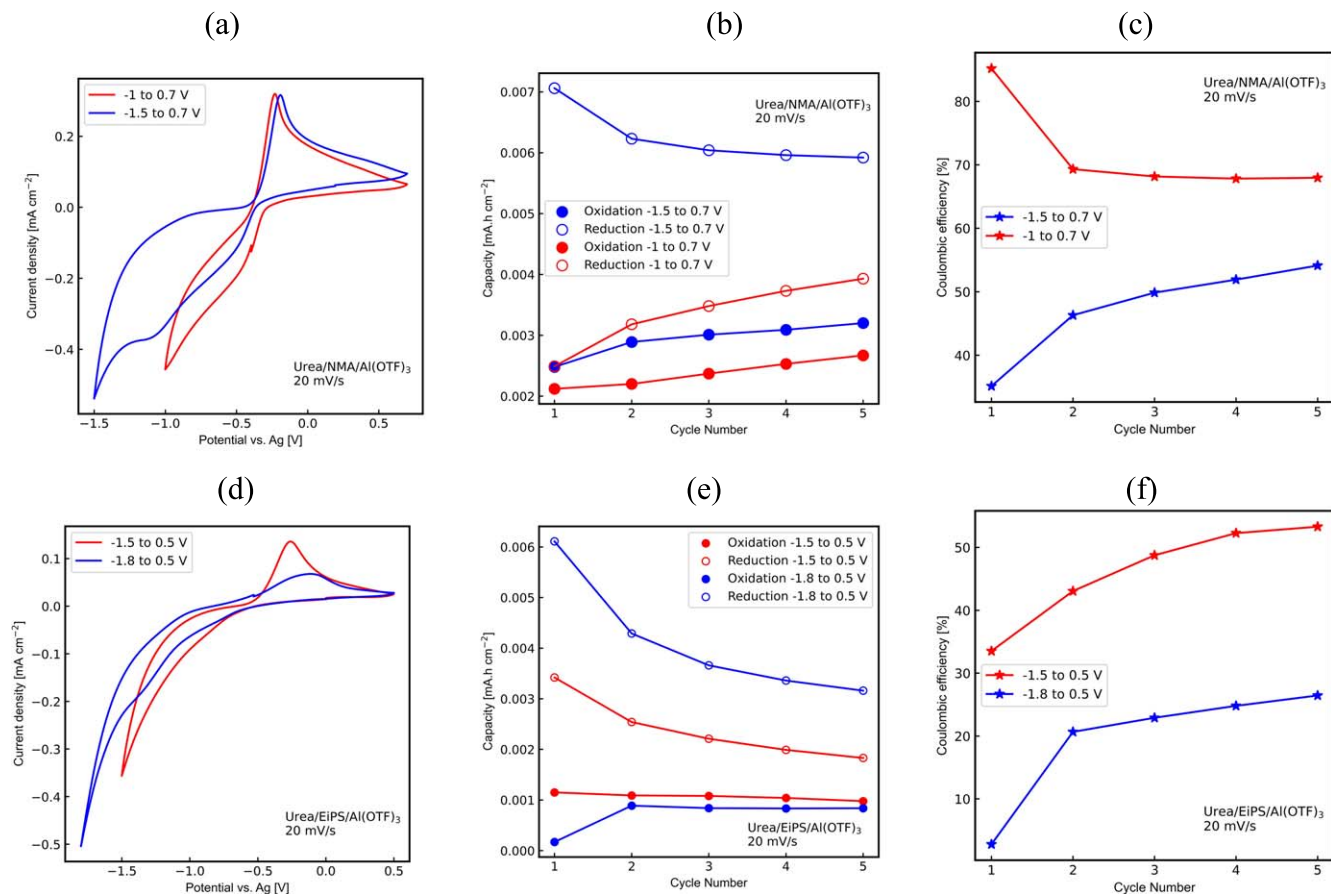


Figure 7. Cyclic voltammograms recorded on a Pt disc as working electrodes vs Ag quasi-reference electrode, oxidation and reduction capacity, and Coulombic efficiency at 20 mV s⁻¹ (a-b-c) in urea/NMA/Al(OTF)₃ at two potential windows -1.5 to 0.7 V and -1 to 0.7 V (d-e-f) in urea/EiPS/Al(OTF)₃ at two potential windows -1.5 to 0.5 V and -1.8 to 0.5 V. The cell used was TSC 1600 closed cell with a Pt as a counter electrode.

Electrochemical characterization of the electrolytes.—The first cyclic voltammetry (CV) curve recorded on a Pt disc electrode in the NMA-based electrolyte agrees with the literature,¹⁶ regardless of having a different cell setup (Fig. 4 cycle 1). However, a shift of the oxidation peak upon cycling is observed, while only one cycle was previously reported in the literature.¹⁶ In order to clarify the reason for the drift of the oxidation peak, a calibration of the Al wire quasi-reference electrode against Ferrocene (used as an internal reference) was performed. Fig. 5a shows that the redox peaks of Ferrocene against Al wire strongly shift to lower potentials by increasing the cycle number over 24 h. This potential drift can be correlated to the surface of the Al quasi-reference electrode, which may change during cycling and in contact with the electrolyte. On the other hand, the measured potential using silver wire as the quasi-reference is very stable during the 24 h (Fig. S5b). It is important to notice that metallic aluminum is always used as a reference electrode in the literature related to Al batteries and the reference calibration is not reported so far. Based on these results, it is clear that the Al quasi-reference electrode is not suitable for studying these electrolytes and an Ag quasi-reference electrode should be a better choice.

The anodic stability of the electrolytes is obtained by LSV measured on Pt and GC discs as working electrodes vs Ag quasi-reference electrode. The cell potential was recorded from the open circuit potential (OCP) to +3 V with scan rates of 10 and 5 mV s⁻¹ till the increase in current was observed. As a criterion, a current of 0.2 mA cm⁻² was chosen to determine the potential limit. Figure 5 shows that the anodic potential limit of the EiPS-based electrolyte is larger than the NMA-based electrolyte independently of the electrode substrate.

As Figs. 6a and 6b show, in Al(OTF)₃-based electrolyte, an oxidation peak appears at -0.2 V vs Ag on Pt electrode. Furthermore,

two different types of Pt substrates, disc, and foil, with electrode surface areas of 0.07 cm² and 0.28 cm², respectively, have been used as working electrodes in the NMA-based electrolyte in two different cell configurations (Fig. 6a and Fig. 10). Figure 6c clearly shows the crucial role of urea: in the absence of urea, the electrochemical reduction is completely disabled and it is clear that the interaction Al-urea is the fundamental factor for Al plating and stripping. Urea plays a fundamental role in the desolvation process (i.e. the weakening of the interaction EiPS—Al³⁺) and, as a result, the reduction of Al³⁺ is hindered without this component. In addition, urea improves the dielectric properties of the electrolyte and consequently increases the ionic conductivity by facilitating the dissociation of Al(OTF)₃.⁵ The dielectric constant (ϵ_r) of the solvent has a direct impact on salt dissociation and ion-ion interactions. Therefore, the degree of salt dissociation depends on the competitive interactions of ion-ion and ion-solvent. The lower dielectric constant of the solvent leads to lower conductivity and, consequently, less salt dissociation. The improvement of Al(OTF)₃ dissociation by adding urea has already been proved with the NMA-based electrolyte.¹⁸ The molar ratio between the solvent and the urea significantly impacts the solvation ability since even a small amount of urea initiates the Al(OTF)₃ dissociation.⁵ Moreover, considering the relatively low dielectric constant of EiPS (55),²⁰ the poor dissociation of Al(OTF)₃ would be improved by adding urea as a substitution for EiPS. The capacities over consecutive CV cycles and coulombic efficiency of both Al(OTF)₃-based electrolytes on Pt electrodes are presented in Figs. S7 and S8. Although an indication of possible plating and stripping can be assumed, the capacities are much smaller as compared with those reported for “standard” AlCl₃/ionic liquid electrolytes.¹⁸ Moreover, the coulombic efficiency is still too low for battery applications.

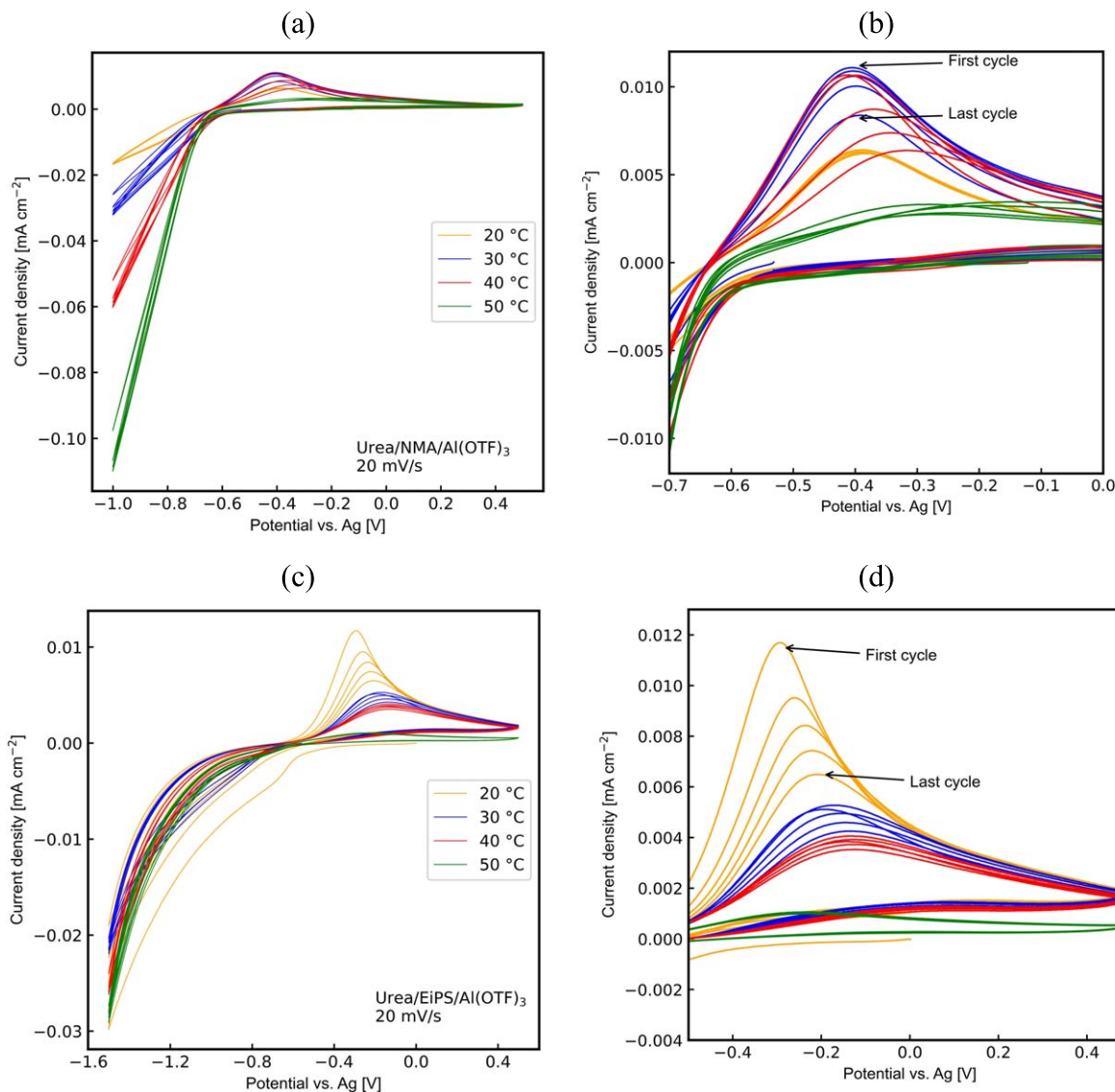


Figure 8. Cyclic voltammograms were recorded on a Pt electrode vs Ag wire quasi-reference electrode at the temperature range of 20 to 50 °C (a-b) in urea/NMA/Al(OTF)₃, and (c-d) in urea/EiPS/Al(OTF)₃. b and d are a magnification of a and c.

The effect of the cathodic potential limit.—The applied voltage range, as an essential factor in the performance of the electrolyte, specifies the limits of electrolyte decomposition and also regulates the possible potential range for the designed reactions. To get more insights about the reversibility of the interest redox reaction, different cathodic potentials with the lower potential limit of -1 V and -1.5 V vs Ag have been applied (Fig. 7). It must be considered that the observed reduction/oxidation current could be due to either Al deposition/dissolution or possible electrolyte decomposition (or to the sum of both reactions).

In general, low coulombic efficiency is a result of undesirable, unwanted, and irreversible reactions that are unrelated to the battery's normal charge and discharge behavior, possibly due to traces of water or to irreversible decomposition of the electrolyte components. Concerning the NMA-based electrolyte, it is known that NMA and urea have strong coordination with Al³⁺ ions, and as a result, a large polarization, i.e., overpotential, is needed for the desolvation process¹⁶ which, in turn, may shift the electrodeposition to lower potentials. The low cycling efficiency can be caused by side

reactions that occur at a larger cathodic limit with the decomposition of the electrolytes. As shown for the 5th cycle in Fig. 7a, for the lower cathodic limit, the reduction reaction has an overpotential, which shows that the reduction is kinetically limited. Accordingly, a lower cut-off potential (-1.5 V) results in a higher capacity. The lower cut-off of -1.5 V induces higher irreversibility and for this reason, the cathodic limit of -1 V has been chosen for further studies (Fig. 7b and 7c). Within the lower potential cut-off of -1 V, the EiPS-based electrolyte shows negligible current density (Fig. S9b); for this reason, it is necessary to decrease the potential further. Fig. 7d shows the 5th CV cycle of the EiPS-based electrolyte with two cathodic limits of -1.5 and -1.8 V. With a cathodic limit of -1.8 V, the irreversibility dramatically increases, leading to a smaller oxidation current. Therefore, for the EiPS-based electrolyte, the optimum cathodic limit can be considered as -1.5 V.

Variation of operative temperature and the critical role of the electrode substrate.—Increasing the temperature generally results in an increase in ion mobility and a decrease in viscosity. Besides, by

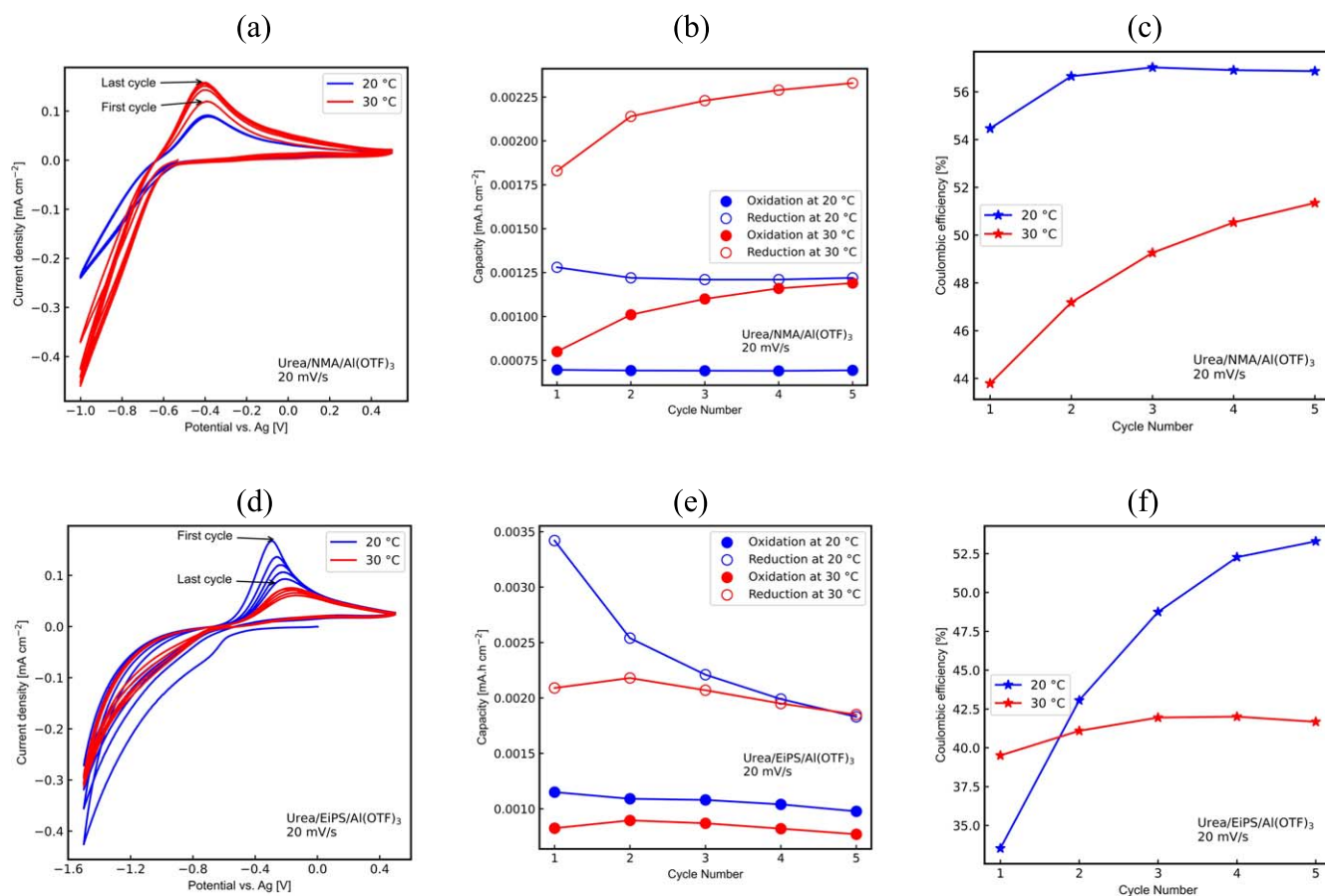


Figure 9. Cyclic voltammograms were recorded on a Pt electrode vs Ag wire quasi-reference electrode at 20 and 30 °C, oxidation and reduction capacity, and Coulombic efficiency at 20 mVs⁻¹ in (a-b-c) urea/NMA/Al(OTF)₃, and (d-e-f) in urea/EiPS/Al(OTF)₃.

increasing the temperature, Al(OTF)₃ dissociation would be facilitated. As shown in Fig. 8, there is a similar trend for both Al(OTF)₃-based electrolytes with the temperature. The rise of the temperature increases the reduction current but hinders the oxidation. Accordingly, by increasing the temperature from 20 to 50 °C, the reduction capacities are higher than oxidation ones (presented in Fig. 8 and Fig. 9), resulting in a lower coulombic efficiency (Fig. S10 and S11). Fig. 9a reveals that the increase of the temperature from 20 to 30 °C reduces the polarization and induces higher reduction/oxidation currents. On the contrary, in the EiPS-based electrolyte, lower reduction/oxidation currents are obtained at 30 °C in comparison to 20 °C (Fig. 9d). As discussed above, due to the high boiling point of EiPS (265 °C), it can be assumed that the EiPS-based electrolyte should have a wider operable temperature window with respect to the NMA-based electrolyte. However, increasing temperature results in lower capacity and coulombic efficiency for both Al(OTF)₃-based electrolytes. It means that the temperature increase affects the kinetic for both the desired redox reaction (i.e., Al plating and stripping) and side (undesired) reactions. As the amount of urea is higher in the EiPS-based electrolyte, the results point towards the decomposition of urea.

Beside the electrochemical behavior of the electrolyte on Pt disc, it is relevant to understand the electrochemical reactions on other metallic substrates. To the best of our knowledge, the electrochemical activity of urea/NMA/Al(OTF)₃ electrolyte¹⁸ has been shown only on Pt electrodes. However, for real battery applications, cheaper and more abundant metal substrates should be considered. It is well known that the advantage of aluminum batteries is the use of metallic aluminum as a negative electrode and it is, therefore,

crucial to evaluate the suitability of such a metal anode with the electrolyte solution. Figures 10a and 10b show the cyclic voltammetry (2nd cycle) of Pt and GC disc electrodes in NMA-based and EiPS-based electrolytes, respectively. Unfortunately, no redox reactions can be observed on substrates such as glassy carbon, Ti, Mo, and Al foils, as shown in Fig. 10c. Cu, as a metal that could possibly form an alloy with Al, has a different behavior. The CVs of the Pt, Cu and Al foil are compared in Fig. 10d. Indeed, Cu foil shows electrochemical activity with a broad reduction peak at -0.4 V vs Ag followed by a cathodic current increase similar to what was obtained on Pt foil. However, the oxidation is shifted at a much higher potential, crossing the limit of the electrolyte oxidative decomposition. The Al foil shows dramatic differences with Cu and Pt: no evidence of electrochemical activity can be observed on the Al foil, excluding any form of possible Al plating and stripping. This finding raises serious questions on the possibility of enabling a non-corrosive Aluminum battery with metallic aluminum as a negative electrode. Two main possibilities could be behind this behavior: 1) the condition of the Al surface (generally covered by an oxide) hinders the plating and stripping, or 2) the reaction observed on the Pt does not involve plating and stripping, but other reactions are instead occurring. Since the overpotential for hydrogen evolution is low at Pt electrode substrates, there is the possibility that the reduction current observed in voltammograms recorded at a Pt electrode originates from the hydrogen evolution by electrochemical reduction of urea.³⁹ In light of these results, we are currently working in our laboratory in these two directions: i) the clarification of the redox reactions occurring on Pt and ii) the modification of the Al surface by pre-treatment methods.

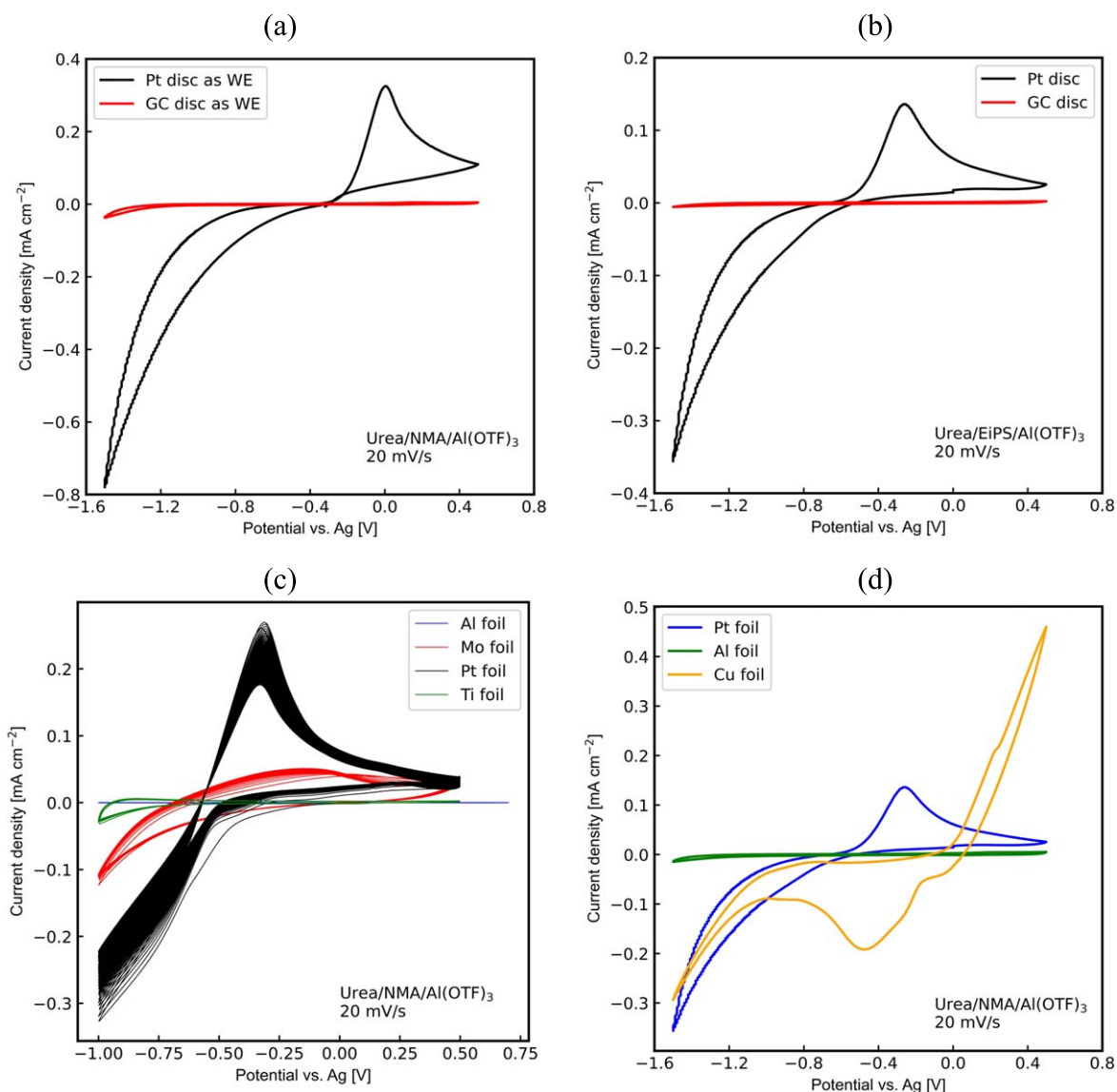


Figure 10. Cyclic voltammograms were recorded on Pt, GC, Ti, Mo, Cu and Al foil in TSC surface cell in (a,c,d) urea/NMA/Al(OTF)₃ and (b) urea/EiPS/Al(OTF)₃ electrolytes. Ag wire is used as quasi-reference electrodes.

Conclusions

To conclude, the electrochemical behavior of the Al(OTF)₃ salt as a suitable and non-corrosive alternative for the acidic AlCl₃ salt has been investigated in two electrolyte compositions with different working electrode substrates at variable temperatures. A new AlCl₃-free electrolyte has been developed by using EiPS, Al(OTF)₃ and urea. It was confirmed that urea plays an important role in electrochemical reduction and ion conductivity, as urea affects not only the desolvation process but also the dielectric properties of the electrolyte. A crucial factor that other researchers in the field should consider is that the electrochemical study of these types of Al(OTF)₃-based electrolytes should be performed not with Al but with Ag quasi-reference electrode, which is a stable reference electrode in AlCl₃-free electrolytes. This study demonstrated that EiPS-based electrolyte has lower ionic conductivity and higher viscosity while having higher thermal stability than NMA-based electrolyte. Moreover, the EiPS solvent can operate at higher anodic potential, thus possibly enabling a higher voltage battery cell as compared to the analog electrolyte with NMA solvent. By studying the temperature's effect on the electrochemical performance of the Al(OTF)₃-based electrolytes, it is proved that ionic conductivity has

a direct relation with temperature. However, besides the increased conductivity with the temperature for both electrolytes, the coulombic efficiency decreases due to low oxidation capacity. Literature routinely presents the room temperature as the ambient temperature where experiments are carried out. In this study, two boundaries for the "room temperature", i.e. 20 and 30 °C are chosen to decipher the sensitivity of electrolytes' electrochemical performance to this 10 °C variation. Less polarization and higher reduction/oxidation currents are observed for the NMA-based electrolyte by increasing the temperature from 20 to 30 °C. Moreover, lower reduction/oxidation currents are obtained at 30 °C compared to 20 °C for the EiPS-based electrolyte. By studying the effect of cathodic potential, it is proved that, for the NMA-based electrolyte, the cathodic limit of -1 V has lower irreversibility compared to -1.5 V. As for the EiPS-based system, the cathodic limit of -1.8 V has lower irreversibility compared to -1.5 V. The crucial finding of this study is the importance of the working electrode's role, which affects Al deposition/dissolution since common metallic working electrodes such as Ti, Al, and Mo foils lack Al deposition. In order to implement Al foil as a practical negative electrode in Al(OTF)₃-based electrolytes, it is necessary to modify the Al foil. Ongoing works in our laboratories are focused on surface

modification to facilitate Al plating and stripping and also on understanding the mechanism of Al plating and stripping and side reactions at the electrode-electrolyte interface during cycling in Al(OTF)₃-based electrolytes.

Acknowledgments

The authors are grateful to Dr. Marcel Drüschler, Dr. Sebastian Kranz from rhd instruments company. The authors would like to thank to thank Dr. Angelina Sarapulova for her scientific help and thank Liuda Mereacre (KIT) for FTIR-TGA measurements. This work contributes to the research performed at CELEST (Center for Electrochemical Energy Storage Ulm-Karlsruhe) and was funded by the German Research Foundation (DFG) under Project ID 390874152 (POLiS Cluster of Excellence). The authors acknowledge project DEAL for open access publishing. Data availability. The data that support the findings of this study are available at <https://doi.org/10.5445/IR/1000156562> and from the corresponding author upon request. Conflict of interest. The authors declare no conflict of interest.

ORCID

Fatemehsadat Rahide  <https://orcid.org/0009-0003-8157-7927>
Sonia Dsoke  <https://orcid.org/0000-0001-9295-2110>

References

1. F. Wu, H. Yang, Y. Bai, and C. Wu, *Adv. Mater.*, **31**, 1806510 (2019).
2. H. Yang et al., *Angew. Chem. Int. Ed.*, **58**, 11978 (2019).
3. S. K. Das, S. Mahapatra, and H. Lahan, *J Mater Chem A Mater*, **5**, 6347 (2017).
4. M. C. Lin et al., *Nature*, **520**, 324 (2015).
5. D. Ma et al., *Energy Environ. Mater.*, **6**, e12301 (2023).
6. T. Schoetz, O. Leung, C. P. de Leon, C. Zaleski, and I. Efimov, *J. Electrochem. Soc.*, **167**, 040516 (2020).
7. R. Böttcher, S. Mai, A. Ispas, and A. Bund, *J. Electrochem. Soc.*, **167**, 102516 (2020).
8. J. K. Chang, S. Y. Chen, W. T. Tsai, M. J. Deng, and I. W. Sun, *Electrochem. Commun.*, **9**, 1602 (2007).
9. B. Craig, T. Schoetz, A. Cruden, and C. Ponce de Leon, *Renew. Sustain. Energy Rev.*, **133** (2020).
10. D. Yuan, J. Zhao, W. Manalastas, S. Kumar, and M. Srinivasan, *Nano Materials Science*, **2**, 248 (2020).
11. C. Ferrara, V. Dall'Asta, V. Berbenni, E. Quartarone, and P. Mustarelli, *J. Phys. Chem. C*, **121**, 26607 (2017).
12. Z. Slim and E. J. Menke, *J. Phys. Chem. C*, **126**, 2365 (2022).
13. H. Wang et al., *ACS Appl Mater Interfaces*, **8**, 27444 (2016).
14. X. Zhang et al., *Adv. Funct. Mater.*, **30**, 2004187 (2020).
15. M. Chiku, S. Matsumura, H. Takeda, E. Higuchi, and H. Inoue, *J. Electrochem. Soc.*, **164**, A1841 (2017).
16. T. Mandai and P. Johansson, *J. Phys. Chem. C*, **120**, 21285 (2016).
17. L. D. Reed, A. Arteaga, and E. J. Menke, *J. Phys. Chem. B*, **119**, 12677 (2015).
18. T. Mandai and P. Johansson, *J Mater Chem A Mater*, **3**, 12230 (2015).
19. L. Legrand, A. Tranchant, and R. Messina, *Electrochim. Acta*, **39**, 1427 (1994).
20. K. Chiba et al., *J. Electrochem. Soc.*, **158**, A872 (2011).
21. S.-J. Kang et al., *Chem. Mater.*, **29**, 3174 (2017).
22. J. Alvarado et al., *Mater. Today*, **21**, 341 (2018).
23. Y. Nakayama et al., *Phys. Chem. Chem. Phys.*, **17**, 5758 (2015).
24. M. Nie and B. L. Lucht, *J. Electrochem. Soc.*, **161**, A1001 (2014).
25. S. K. Das, D. Majhi, P. K. Sahu, and M. Sarkar, *RSC Adv.*, **5**, 41585 (2015).
26. C. Schütter, A. Bothe, and A. Balducci, *Electrochim. Acta*, **331**, 135421 (2020).
27. N. S. V. Narayanan, B. V. Ashok Raj, and S. Sampath, *J. Power Sources*, **195**, 4356 (2010).
28. H. Chaurasia et al., *New J. Chem.*, **43**, 1900 (2019).
29. A. K. Lyashchenko et al., *Russ. J. Inorg. Chem.*, **64**, 924 (2019).
30. M. F. Brigatti, A. Laurora, D. Malferrari, L. Medici, and L. Poppi, *Appl. Clay Sci.*, **30**, 21 (2005).
31. B. Huber and M. Drüschler, *Determination of the temperature-dependent conductivity of a lithium-ion battery electrolyte by means of EIS*, rhd instruments GmbH & Co. KG (2020), (downloadable at: <https://rhd-instruments.de/en/support/downloads>).
32. J. Świergiel and J. Jadżyn, *J. Chem. Eng. Data*, **54**, 2296 (2009).
33. R. Zhang, G. Zhao, and W. Wu, *Chin. J. Chem. Phys.*, **22**, 511 (2009).
34. J. K. Carr, L. E. Buchanan, J. R. Schmidt, M. T. Zanni, and J. L. Skinner, *J. Phys. Chem. B*, **117**, 13291 (2013).
35. W. Peters, H. T. Duong, S. Lee, and J.-F. Drillet, *Phys. Chem. Chem. Phys.*, **23**, 21923 (2021).
36. M. A. Czarnecki and K. Z. Haufa, *J. Phys. Chem. A*, **109**, 1015 (2005).
37. P. M. Schaber et al., *Thermochim. Acta*, **424**, 131 (2004).
38. Q. Li et al., *Carbohydr Polym.*, **195**, 288 (2018).
39. T. Tsuda, T. Tomioka, and C. L. Hussey, *Chem. Commun.*, **2908**, 2908 (2008).